

THE UNIVERSITY OF MICHIGAN
INDUSTRY PROGRAM OF THE COLLEGE ENGINEERING

BEHAVIOR OF AN INELASTIC BUCKLING MODEL
BETWEEN THE TANGENT MODULUS AND SHANLEY LOADS

Bruce G. Johnston

June, 1961

IP-523

LIST OF FIGURES

<u>Figure</u>		<u>Page</u>
1	Evolution of the Column Formula.....	3
2	Inelastic Stress, Strain, and Tangent Modulus Relationships.....	9
3	Buckling Model.....	11
4	Stress Distribution Just Above the Tangent Modulus Load.....	11
5	Strain Increments Between N-1 and N Equilibrium Positions.....	16
6	Approximation to Non-Linear Stress Distribution.....	16
7	Bent E uilibrium Configuration.....	16
8	Stress Distributions $\sigma_T < \sigma_{AVG} < \sigma_M$ L = 16".....	19
9	Stress Distributions $\sigma_T < \sigma_{AVG} < \sigma_M$ L = 30".....	20
10	Stress Distributions $\sigma_T < \sigma_{AVG} < \sigma_M$ L = 46".....	21
11	Lateral Deflection vs. Axial Load for Various Length Struts.....	24
12	Lateral Deflection vs. Axial Load With Strut Held Straight to Various Stresses Above Tangent Modulus Load.....	26
13	Lateral Deflection vs. Axial Load for Assumption of Constant E_T Above σ_T	28
14	"Column" - Strength Curves.....	30

TABLE OF CONTENTS

	<u>Page</u>
1. Introduction.....	1
2. Evaluation of the Shanley Load.....	7
3. Results of the Simulated Tests.....	18
3.1 Stress Distribution.....	18
3.2 Load Deflection Curves.....	23
3.3 Column Strength Curve.....	29
4. Summary.....	29
5. References.....	33

1. Introduction

This report describes in detail the inelastic buckling behavior of a concentrically loaded strut having a reduced rectangular cross section as a mid-section. The buckling model is identical to that originally used by Shanley⁽¹⁾ to support his concepts except that in the Shanley model two localized points of area were assumed whereas in the present model a solid rectangular cross section is introduced which permits a detailed exploration of stress distribution across the section. One purpose of this paper is to determine quantitatively at various load levels the stress distributions that were described intuitively by Shanley in his original paper. The behavior of struts held so as to remain straight above the tangent modulus load will also be studied, as well as other aspects of behavior that may lead to a better appreciation and understanding of inelastic buckling behavior.

The results presented herein pertain to a series of simulated experiments on structural aluminum alloy struts of various lengths. Stress distribution across the section, load deflection curves, and other information are determined by use of the IBM 704 computer. There

* Professor of Structural Engineering, Civil Engineering Department, University of Michigan, Ann Arbor, Michigan.

are many advantages in simulated tests, carried out with the aid of a computer, in comparison with real tests in an actual testing machine. No machining is involved, no materials need be acquired, and there is no scatter in the test results. Moreover, the precision of results, although based on a simulated and idealized material, permits a study of details of behavior that is not possible in ordinary laboratory tests. It would be impossible to duplicate completely the observations that may be made on the basis of the simulated tests reported in this paper. The Shanley load is determined quantitatively and is defined as the maximum load that is attained by a concentrically loaded strut that starts to bend at the tangent modulus load.

In discussing properly the work of Shanley it is essential that the development of the Euler formula and its modifications be reviewed over the period of 203 years between it and Shanley's work. An excellent source for such a review has been provided by N. J. Hoff.⁽²⁾ Figure 1 summarizes the principal developments in outline form. In 1744 Euler presented his evaluation of the average stress at which a slender axially loaded strut of constant cross section will develop bifurcation of equilibrium positions at a constant load. For many years Euler's formula was not generally applied to actual design since proof tests of structures indicated that columns frequently failed below the Euler load. In 1889 Considere indicated why Euler's formula had not been more useful to engineers. He conducted a series of 32 column tests and suggested that if buckling occurred above the proportional limit the elastic modulus "E" should be replaced in the Euler

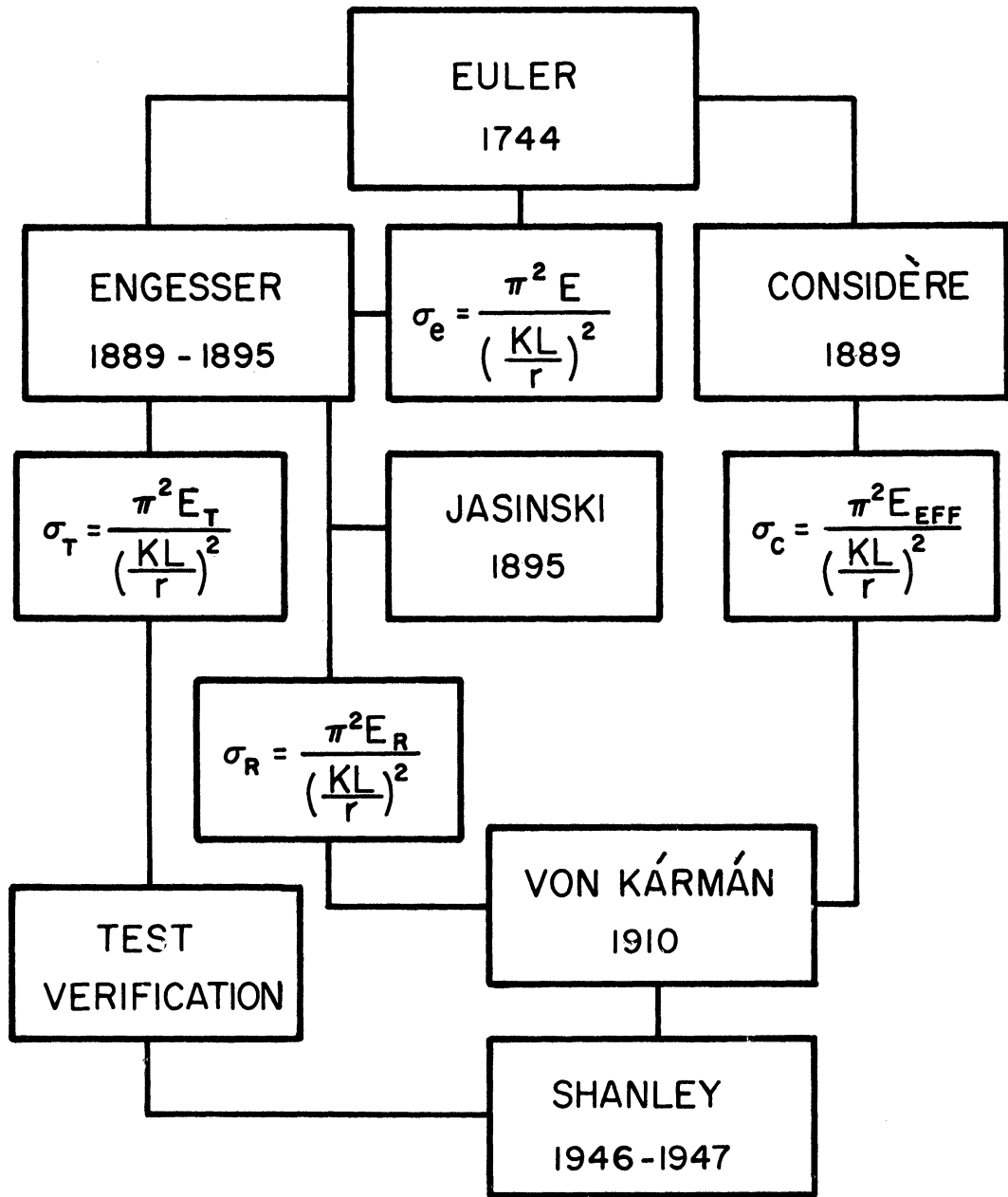


Figure 1. Evolution of the Column Formula.

formula by an " E_{eff} ". He correctly stated that this effective modulus should be somewhere between the elastic modulus E and the tangent modulus E_t .

Independently of Considère, during the same year of 1889, Engesser suggested that column strength in the inelastic range might be obtained by the substitution of E_t in place of E in the Euler formula. This is known today as the "tangent modulus formula" and has been accepted recently by Column Research Council⁽³⁾ as the "proper basis for the establishment of working load formulas" for both ferrous and non-ferrous metals.

In 1895 Jasinski suggested that there was an apparent mistake in Engesser's formula in that the nonreversible characteristic of the stress-strain diagram in the inelastic range should be considered as had been done in a very general way by Considère. Engesser proceeded within the same year to produce a "corrected" general formula for a "reduced modulus" and he stated that this reduced modulus depended not only upon " E_t " and " E " but on the shape of the cross section as well.

In 1910 vonKármán derived explicit expressions for the "reduced modulus" for both the rectangular and the idealized H-section columns. For the rectangle

$$E_R = \frac{4E E_t}{(\sqrt{E} + \sqrt{E_t})^2} \quad (1)$$

The reduced modulus is also called, appropriately, the "double modulus" and for about 35 years subsequent to vonKármán's work a controversy was waged over the comparative merits of the tangent modulus and double modulus column formulas. From the classical

instability concept the double modulus theory was correct since it indicated the load at which a perfectly straight and centrally loaded column could have neighboring equilibrium configurations with no change in load. This is identical in concept to the Euler load in the elastic buckling range. However, many experimenters found that columns tested in the laboratory with utmost care usually buckled at loads just slightly above the tangent modulus load. For example, very careful tests were made in the 1930's by the Aluminum Research Laboratories.⁽⁴⁾ One of their conclusions was: "The test data presented herein are in close agreement with Engesser's formula...". By this was meant the tangent modulus formula, even though Engesser had himself renounced it.

In 1946 Shanley⁽⁵⁾ reconciled the controversy between the proponents of the tangent modulus and the double or reduced modulus theories. His explanation now seems simple in retrospect. Shanley showed that since it was obviously possible for a column to bend simultaneously with increasing axial load, without strain reversal, it was reasonable to conclude that such bending would start at the tangent modulus load. Thus, normally, for the usual stress-strain curves, the double modulus load never could be reached because it is based on equilibrium configurations in the neighborhood of a perfectly straight column. In a letter published jointly with the 1947 Shanley paper, vonKármán⁽¹⁾ redefined the tangent modulus load in a way that may be paraphrased as follows:

"The tangent modulus load is the smallest value of the axial load at which bifurcation of the equilibrium positions can occur regardless of

In 1950 Lin⁽⁷⁾ presented results of his inelastic analysis of a slightly curved column, including effects of strain reversal, considering a rectangular section with distributed area.

2. Evaluation of the Shanley Load

A numerical procedure will be presented for the evaluation of the Shanley load. Although the method is applied herein to an inelastic buckling model with only a limited section at the center that undergoes bending, the method may readily be extended to more realistic columns with variable cross section. A digital computer will be required in such an undertaking and at each successive equilibrium evaluation, the column configuration by the Newmark⁽⁸⁾ numerical procedure will be determined.

After bending starts at the tangent modulus load, successive deflected equilibrium configurations must be established for which the increased column load and increased internal bending resistance are in equilibrium. The resisting internal moment and thrust resultants are determined by a pattern of stress across the cross section of the column that changes shape with each load increment. The calculation of a sequence of equilibrium positions for a succession of small load increments is essential because over an appreciable portion of the column cross section the material experiences first an increase in stress under a continually changing tangent modulus followed by a regression of strain which produces a stress reduction as determined by the elastic modulus.

The successive equilibrium configurations must be determined very precisely for a sequence of very small increments of unit rotation with consideration of the continually changing values of tangent modulus. It is not practicable to use values of E_t obtained graphically from an experimental curve. It is necessary to use a mathematical expression which will simulate consistently both the tangent modulus and compressive stress as a function of strain to as great a numerical precision as may be required to give consistent numerical results. Duberg and Wilder⁽⁶⁾ used the generalized stress-strain curves of Ramberg and Osgood.⁽⁹⁾ These provide a wide variety of shapes with the added advantage that each curve throughout the entire range is represented by a single expression. The Ramberg-Osgood curves could readily be adapted to the procedure employed herein, but it was desired to take a very close look at the behavior near the transition from elastic to inelastic behavior. The Ramberg-Osgood curves have no truly elastic range and were not used in the present study.

The simulated properties for computer analysis correspond closely to the minimum properties guaranteed by the Aluminum Company of America for aluminum alloy 2014-T6. The guaranteed minimum properties are shown by dashed lines in Figure 2 and the simulated properties represented by various empirical relationships within the ranges indicated are shown on the same figure. The equations for stress and tangent modulus within the range $0.0032 < \epsilon < 0.0062$ are given by Equations 2 and 3, respectively, as follows:

$$\sigma = 14.08 + 6200 \epsilon + 4.34175 \sin \left[\frac{\pi(\epsilon - 0.0032)}{0.0031} \right] \quad (2)$$

$$E_t = \frac{d\sigma}{d\epsilon} = 6200 + 4400 \cos \left[\frac{\pi(\epsilon - 0.0032)}{0.0031} \right] \quad (3)$$

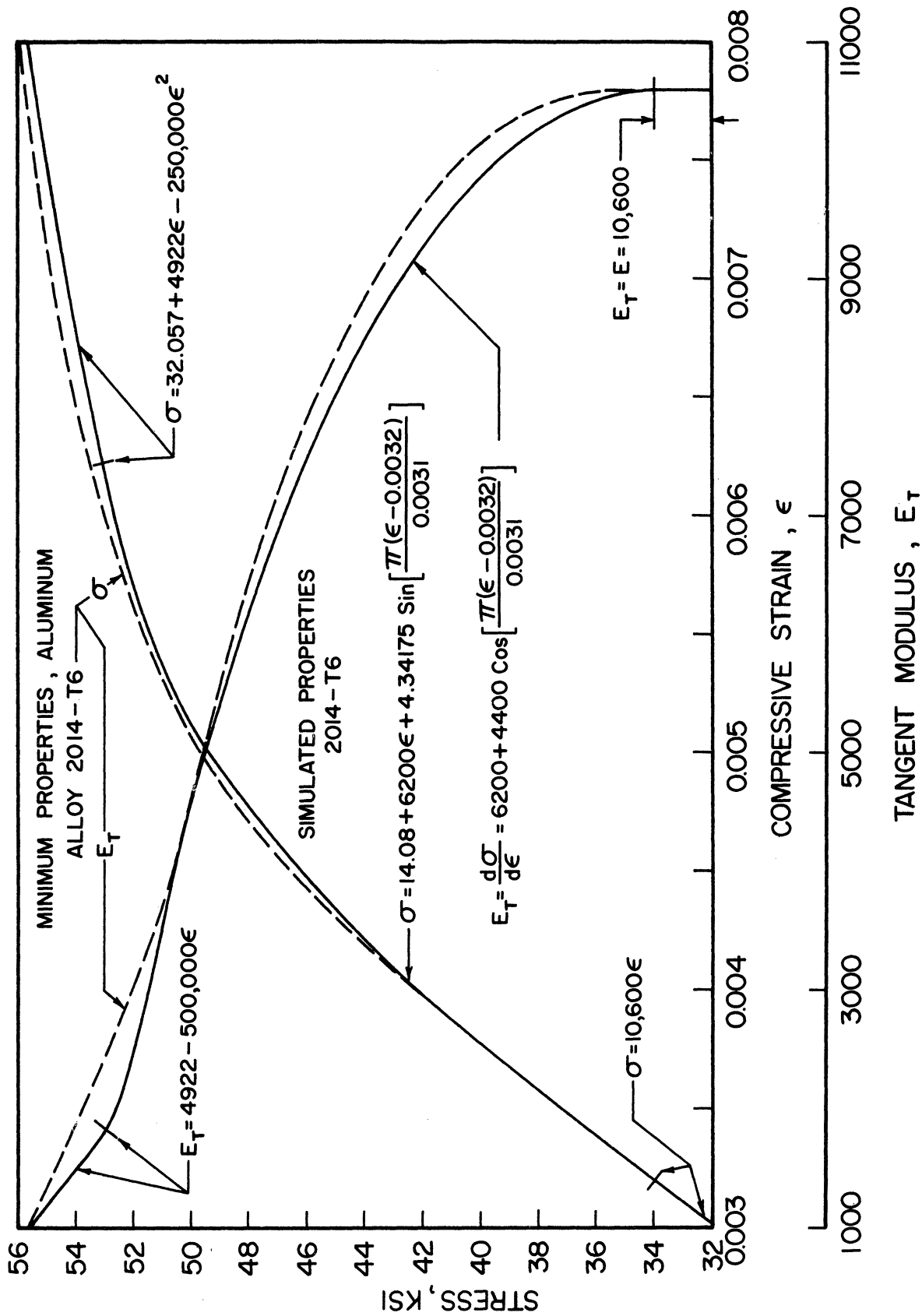


Figure 2. Inelastic Stress, Strain, and Tangent Modulus Relationships.

It is assumed that for stresses up to 33.92 ksi that the material is elastic with an elastic modulus of 10,600 kips per inch². For $\epsilon > 0.0062$ additional expressions for σ and E_t are indicated on Figure 2.

The buckling model to be considered herein is shown in Figure 3. The central non-rigid segment is of square cross section with breadth H and length A. It is assumed that during bending the segment of length A has a parabolic bent shape for which a simple equilibrium evaluation in the deflected position, using the moment area procedure, gives the following buckling stress in the elastic range.

$$\sigma_c = \frac{EH^2}{A \left[6B + A \frac{(B + \frac{5}{16} A)}{(B + \frac{A}{4})} \right]} \quad (4)$$

Equation 4 for this buckling model corresponds to the Euler buckling stress for a column of uniform cross section. Equation 4 is an approximation and, if $B = 0$, in which case the buckling model becomes a column of uniform square cross section with the length A, the buckling stress is

$$\sigma_c = \frac{0.8E}{\left(\frac{A}{H}\right)^2} \quad (5)$$

If Equation 5 is written in terms of the radius of gyration of the cross section $R = H/\sqrt{12}$ we have the following approximation of the Euler buckling load for a square column of length A.

$$\sigma_c = \frac{9.6E}{\left(\frac{A}{R}\right)^2} \quad (6)$$

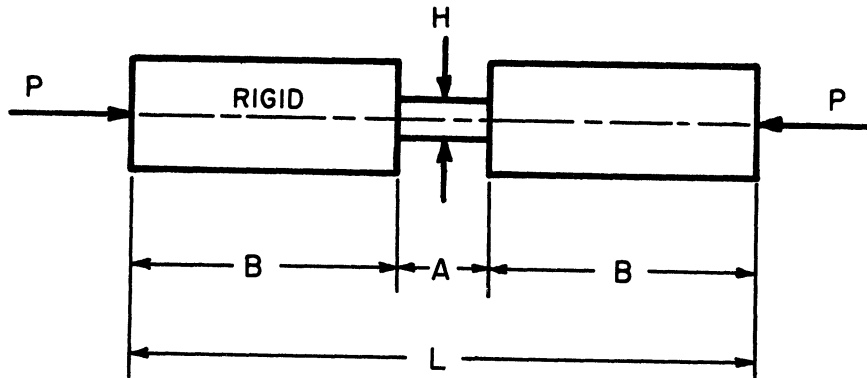


Figure 3. Buckling Model.

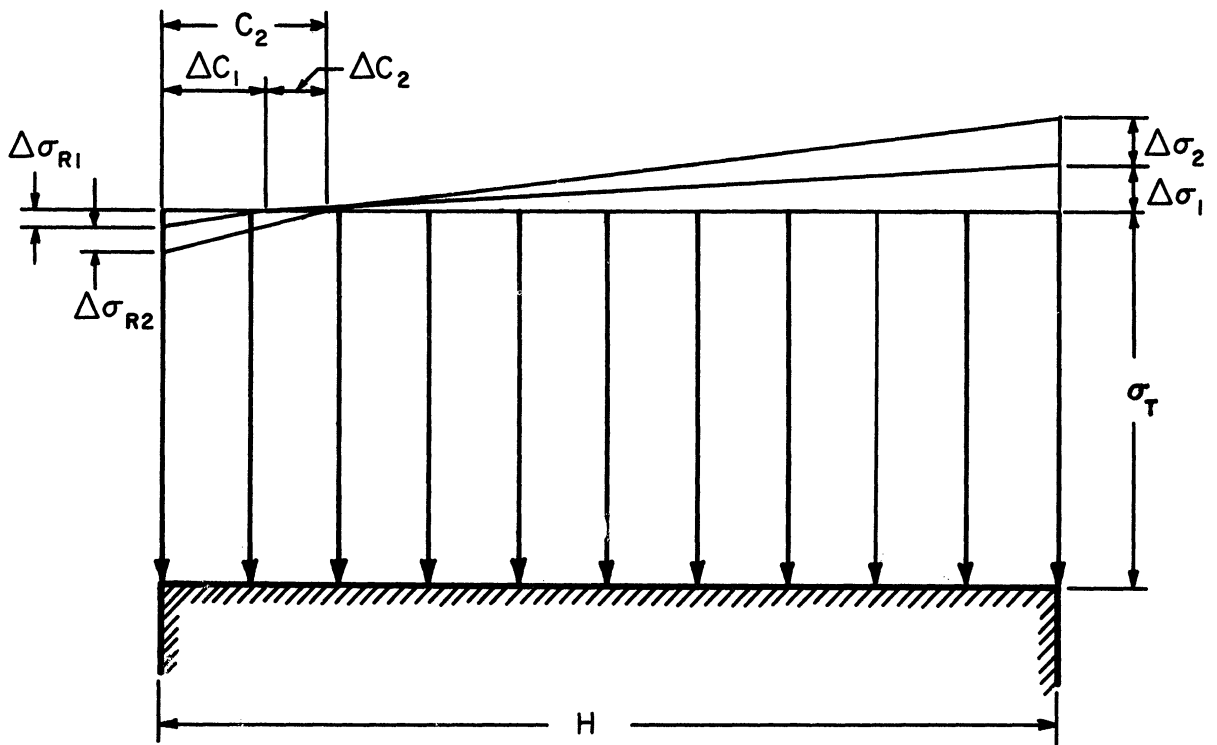


Figure 4. Stress Distribution Just Above the Tangent Modulus Load.

The exact Euler buckling formula for the pin ended case is the well known Equation 7 with L designated as the length of the column.

$$\sigma_c = \frac{\pi^2 E}{\left(\frac{L}{R}\right)^2} \quad (7)$$

Although the buckling load by Equation 6 is 2.7% less than the correct value by Equation 7 the approximation in the case of the buckling model will improve and the error grow less as the length of the rigid segments increases. If the elastic modulus E in Equation 4 is replaced by the tangent modulus E_t (corresponding to the identical stress level) the formula will correspond to the tangent modulus formula for column buckling. Similarly, if the reduced double modulus given by Equation 1 is substituted in Equation 4 the reduced modulus buckling stress will be obtained. In calculating E_R the value of E_t corresponds, of course, to the higher reduced modulus load σ_R .

The initial changes in stress distribution just above the tangent modulus load will now be discussed. Figure 4 shows the stress distribution as uniform at σ_T over the cross section.

If additional load above the tangent modulus load is now applied to the "inelastic buckling model" or "strut", as it hereinafter will be called, the strut will start to bend. This bending will cause the stress on one side, as shown, to increase by $\Delta\sigma_1$. The subscript denotes this as the first increment of stress above the tangent modulus value. Now if $\Delta\sigma_1$ were thought of as an infinitesimal quantity $d\sigma$, in the limit, just as bending was initiated, in the limit there would be no change in column load and the tangent modulus would

apply over the entire cross section. There would be no strain regression anywhere and ΔC_1 , as shown in the figure, would be zero. If, however, $\Delta\sigma_1$ is an actual finite difference in stress level there will be a finite increase in column load above the tangent modulus load. If the tangent modulus governed the stress-strain relation over the entire cross section any increase in load above the tangent modulus load would be supercritical since the tangent modulus load itself would be the maximum buckling load capacity if the tangent modulus were to govern the stress-strain relationship over the entire cross section. Thus if a finite $\Delta\phi$ is thought of as representing the first increment of unit curvature, the strut cross section at the point of maximum deflection will have to develop enough bending moment resistance to be in equilibrium with the resultant moment due to the external load P , increased by ΔP_1 . This increase in bending resistance can occur only if some strain reversal takes place. Thus, if the tangent modulus stress is thought of as a new reference for stress changes, there will be in effect a movement of the "neutral axis" inward from the edge of the cross section by an amount ΔC_1 and there will be a stress regression on this convex side of the column as indicated by $\Delta\sigma_{R1}$.

If a second increment of rotation is permitted, corresponding to a further increase in axial column load and increase in internal resisting moment, there will be a further movement during this second increment somewhat smaller than the first one, as indicated in Figure 4 by ΔC_2 . This is the only way in which a positive increment in moment can be developed to offset the increase of external moment caused by

the axial load $P + \Delta P_1 + \Delta P_2$. The increase in compressive stress indicated by $\Delta\sigma_2$ will be less than $\Delta\sigma_1$ because we are now moving out along a typical inelastic stress-strain curve in which the second derivative of σ with respect to ϵ is everywhere negative. In carrying out calculations of this type it will be assumed that the average tangent modulus during each increment of rotation governs the increase in stress that occurs during that particular rotation and load increment.

It is to be noted that within the region "C" the stress will first increase according to the local tangent modulus and thereafter decrease according to the elastic modulus.

Consider now the change in rotation and its effect on axial load, moment, and "C" for the Nth increment of rotation, shown in Figure 5 as the difference between the strain distribution at increment N and at the preceding increment N-1. Although there will be an appreciable variation in tangent modulus over the cross section of the strut, the increments of load and moment during any particular rotation increment can be closely approximated if the tangent modulus is determined by a single value that decreases with each successive rotational increment but is determined by the actual strain one-quarter of the distance (H-C) in from the concave side of the column. If the stress varied linearly throughout the increasing range this would be the location at which the total force increment could be considered as concentrated and this will give a close approximation for the non-linear distribution that actually exists. Thus, referring to Figure 5,

the strain that will be used as an index of the changing tangent modulus will be determined by Equation 8 as follows.

$$\epsilon_{N(AVG)} = \epsilon_T + 0.75(N - 0.5)(H - C_{N-1})\Delta\phi \quad (8)$$

The actual strain distribution over the entire cross section will be assumed to vary linearly and this index strain given by Equation 8 is merely for the purpose of evaluating a tangent modulus for which an assumed triangular distribution of increased compressive stress is assumed satisfactorily to represent the actual non-linear distribution of increased compressive stress for that particular load. The foregoing explanation is illustrated graphically in Figure 6, which shows a possible stress distribution at a particular bent equilibrium position as a solid line. In the analysis the curved solid line portion in the right portion of the stress distribution is replaced by the dashed line which intersects the curved line at the location where the index strain has been determined.

Referring now again to Figure 5 the magnitude of axial force, moment, and "C" will be determined after the Nth $\Delta\phi$ that is introduced as a result of bending that commences at the tangent modulus load.

Thus,

$$P_N = P_{N-1} + (\Delta P)_N \quad (9)$$

$$M_N = M_{N-1} + (\Delta M)_N \quad (10)$$

$$C_N = C_{N-1} + (\Delta C)_N \quad (11)$$

Each $\Delta\phi$ during a particular numeric step will be arbitrarily the same, thus ϕ_N may be considered as the independent variable in the

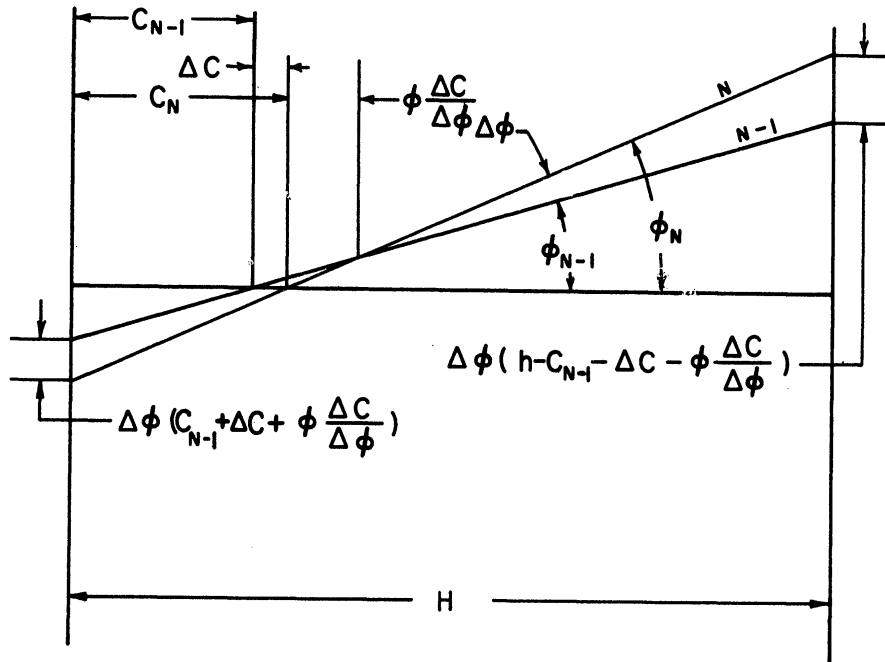


Figure 5 Strain Increments Between N-1 and N Equilibrium Positions.

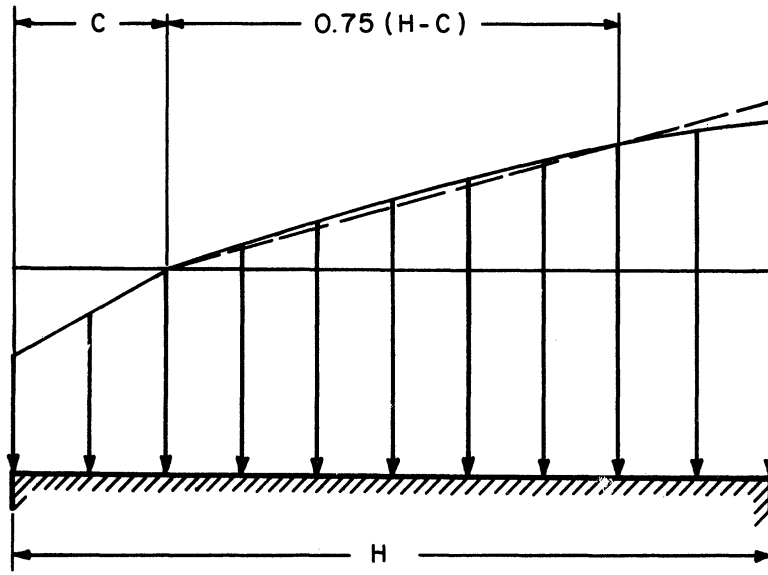


Figure 6. Approximation to Non-Linear Stress Distribution.

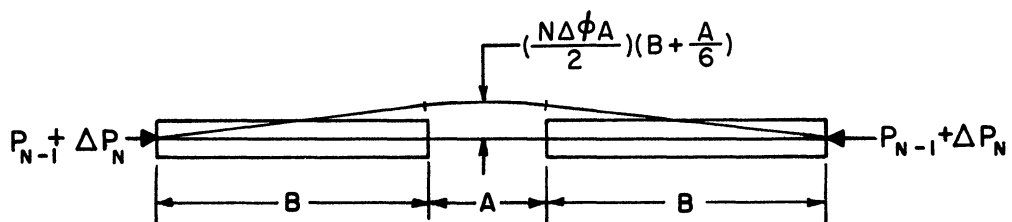


Figure 7. Bent Equilibrium Configuration.

solution of a particular equilibrium condition and

$$\phi_N = N\Delta\phi \quad (12)$$

On the basis of the arbitrary rotation $\Delta\phi$, as shown in Figure 5, the following equations may be written for ΔP_N and ΔM_N .

$$\begin{aligned} \Delta P_N = \frac{H\Delta\phi}{2} & \left[(H-C_{N-1})^2 E_{TN} - C_{N-1}^2 E - 2N \left[(H-C_{N-1}) E_{TN} + C_{N-1} E \right] \Delta C_N \right. \\ & \left. - N^2 (E-E_{TN}) \overline{\Delta C_N^2} \right] \end{aligned} \quad (13)$$

$$\begin{aligned} \Delta M_N = \frac{H\Delta\phi}{12} & \left[(H-C_{N-1})^2 (H+2C_{N-1}) E_{TN} + C_{N-1}^2 (3H-2C_{N-1}) E \right. \\ & + 6NC_{N-1} (H-C_{N-1}) (E-E_{TN}) \Delta C_N + 3N^2 (H-2C_{N-1}) (E-E_{TN}) \overline{\Delta C_N^2} \\ & \left. - 2N^3 (E-E_{TN}) \overline{\Delta C_N^3} \right] \end{aligned} \quad (14)$$

In Equation 13 values of C_{N-1} will have been determined in the preceding step and E_{TN} will be determined in accordance with the index strain by Equation 8. The same is true for Equation 14. Thus the only unknown quantity in Equations 13 and 14 is ΔC_N which appears up to the third power. For very small values of N , when the strut just starts to bend, ΔC_N may be relatively large and as bending proceeds the quantity $N\Delta C_N$ increases. It will be noted that in every term in which ΔC_N appears it is multiplied by N .

Equations 13 and 14 are combined into a single equation in terms of ΔC_N by means of the equilibrium equation for the N th equilibrium position which may be written:

$$(P_{N-1} + \Delta P_N) \left[\frac{N\Delta\phi A}{2} \left(B + \frac{A}{6} \right) \right] = M_{N-1} + \Delta M_N \quad (15)$$

In Equation 15 the quantity in brackets to the left of the equal sign is the maximum deflection at the center line of the column. The equilibrium condition that determines ΔC_N is also illustrated in Figure 7. The solution of the cubic equation in ΔC that results from the combination of Equations 13, 14, and 15 was carried out with the aid of the IBM 704 computer at the University of Michigan utilizing MAD (Michigan Algorithm Decoder) Programming. The work of programming and the carrying out of all details of the actual numeric solution were handled by Mr. Rafi Hariri, a graduate student at the University of Michigan, for course credit in structural research.

3. Results of the Simulated Tests

Typical results of certain of the simulated tests carried out by means of the computer solution will now be presented and discussed.

In the numerical example used in the simulated tests dimension A (Figure 3) was held constant at 2 inches and dimension H at 1 inch. Thus the reduced section has an area of 1 inch square and the total strut load is always identical with the average stress on the reduced section. Dimension B was varied in increments up to the value that would result in elastic buckling.

3.1 Stress Distribution

The stress distributions across the breadth of the reduced section of the strut at increasing loads are shown in Figures 8, 9, and 10, typical of short, intermediate, and long strut behavior. In

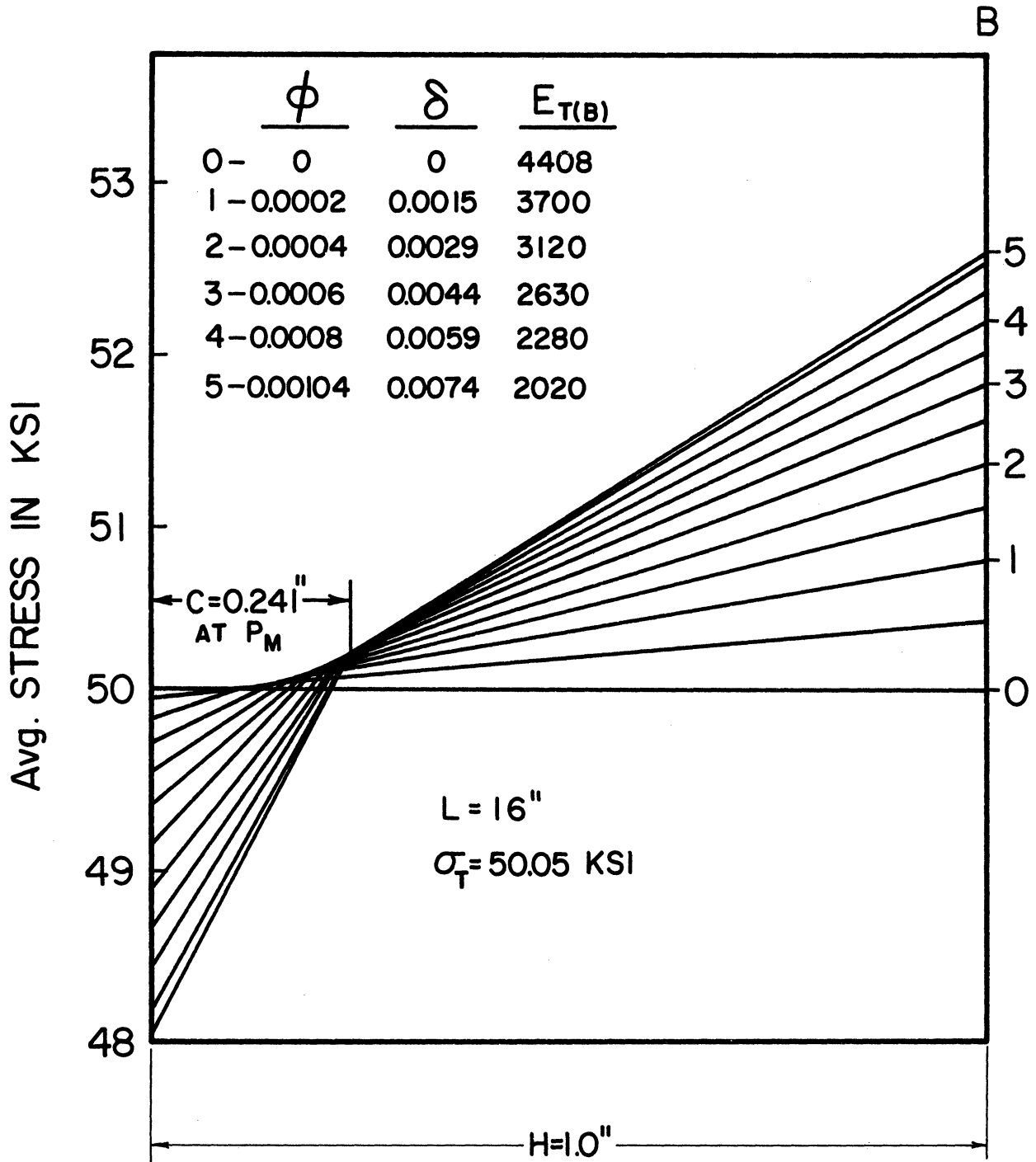


Figure 8. Stress Distributions $\sigma_T < \sigma_{AVG} < \sigma_M$
 $L = 16''$.

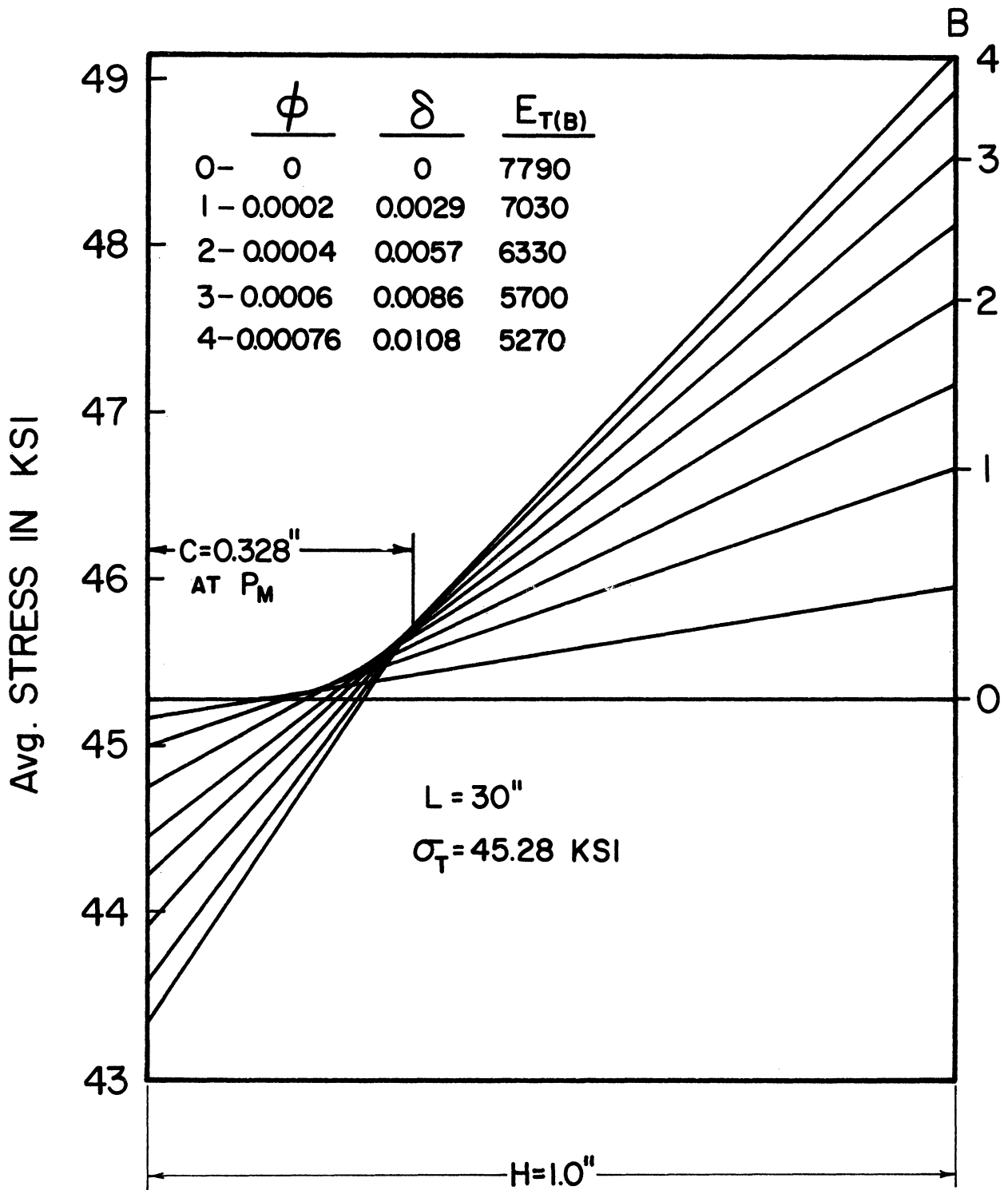


Figure 9. Stress Distributions $\sigma_T < \sigma_{AVG} < \sigma_M$
 $L = 30''$.

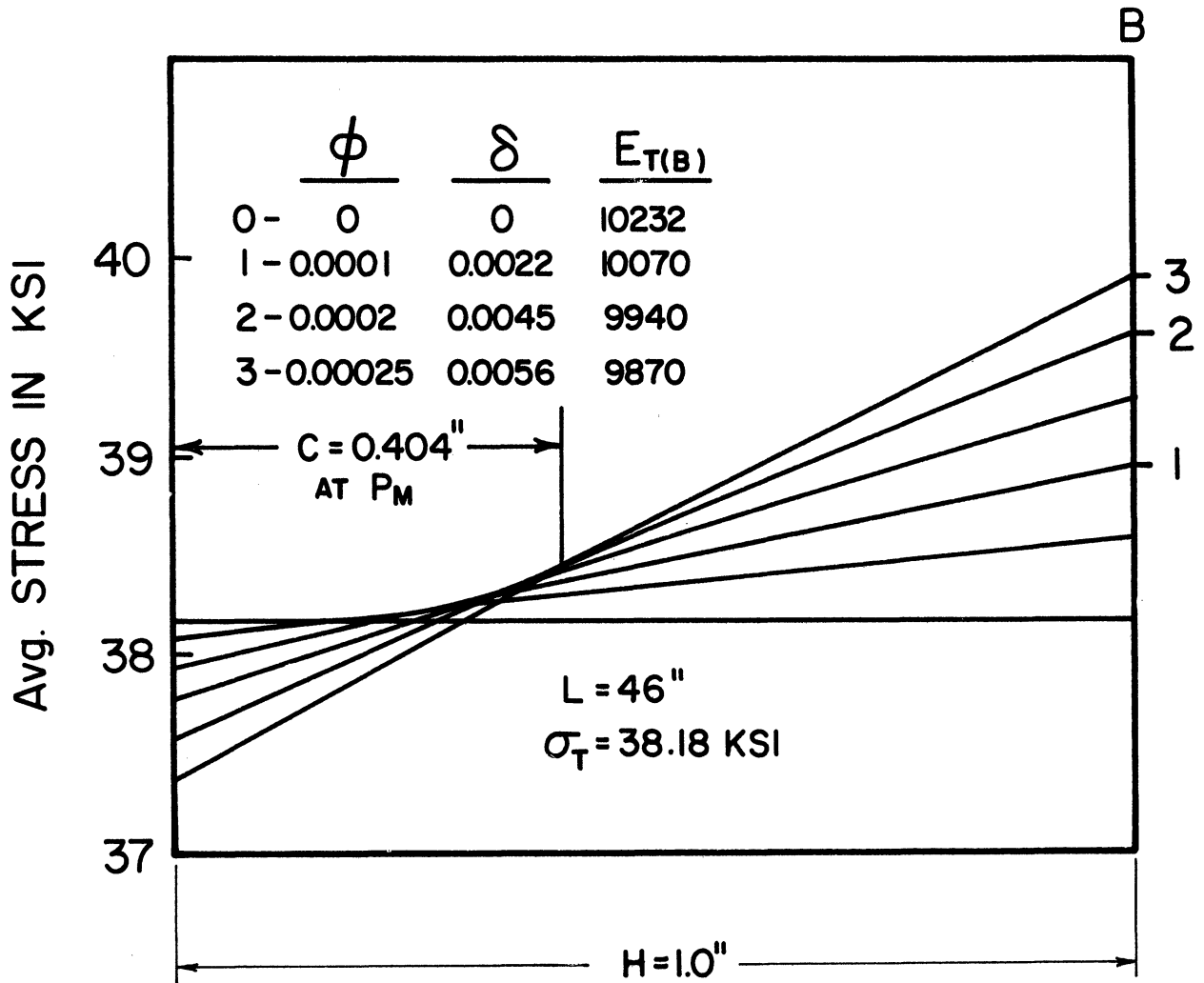


Figure 10. Stress Distributions $\sigma_T < \sigma_{AVG} < \sigma_M$
 $L = 46''$.

Figure 8 the space between each of the stress distribution lines covers ten different equilibrium evaluations at successively increasing loads. Thus, the $\Delta\phi$ used in the determinations of Figure 8 was 0.00001 radians whereas the plotted lines are for a $\Delta\phi$ of 0.0001 radians. As an indication of the fact that $\Delta\phi$ was taken sufficiently small the following tabulation shows results for $L = 43$ inches for various $\Delta\phi$'s as follows:

$\Delta\phi$	Calculated Maximum or Shanley Load in Kips per Sq. In.
0.000002	39.4570
0.000005	39.4566
0.000010	39.4557

It is obvious that in the range of $\Delta\phi$'s that were actually used in determining the Shanley loads the cited value of 0.00001 gave satisfactory accuracy.

Referring again to Figure 8, the gradual inward movement of C is noted, reaching a maximum of 0.241 inches at P_m (the Shanley load). There is a marked reduction in the index tangent modulus E_t . This demonstrates the necessity of considering the progressive change in tangent modulus as bending proceeds above the tangent modulus load. Also to be noted is the very small deflection in comparison with the column length at which the Shanley load is reached. The maximum lateral deflection for this strut at the maximum load is less than one thousandth of the length of the strut. Although the constriction in

the chosen model tends to accentuate these effects, the model is most nearly similar to an actual column in the short length range where the effects are most pronounced.

Figure 9 presents the simulated test stress distributions for an intermediate length of a strut. The inward extent of region C is greater than in Figure 8. The maximum deflection is considerably greater than for Figure 8 at the maximum load but is still less than one thousandth of the strut length. The variation of E_t during bending above the tangent modulus load is large but not so large as in the shorter strut.

Figure 10 is for a relatively long strut that buckles just above the proportional limit. The tangent modulus at this load is very nearly the same as for the elastic range. It is to be noted that the maximum extent of C at maximum load is more than 80% of the way into the center of the column and that the deflection at maximum load is less in proportion to the length of the column than in the previous case. Obviously, in the elastic range there will be no load increment as buckling will occur at constant load and C will not move inward gradually but will be 0.5 at all times.

3.2 Load Deflection Curves

Figure 11 shows typical load vs. lateral deflection curves plotted from the tangent modulus load out to the maximum or Shanley load for eight simulated tests of different strut lengths. The dashed line shows the limit of lateral deflections out to the maximum load. The deflection is zero at the proportional limit, below which elastic

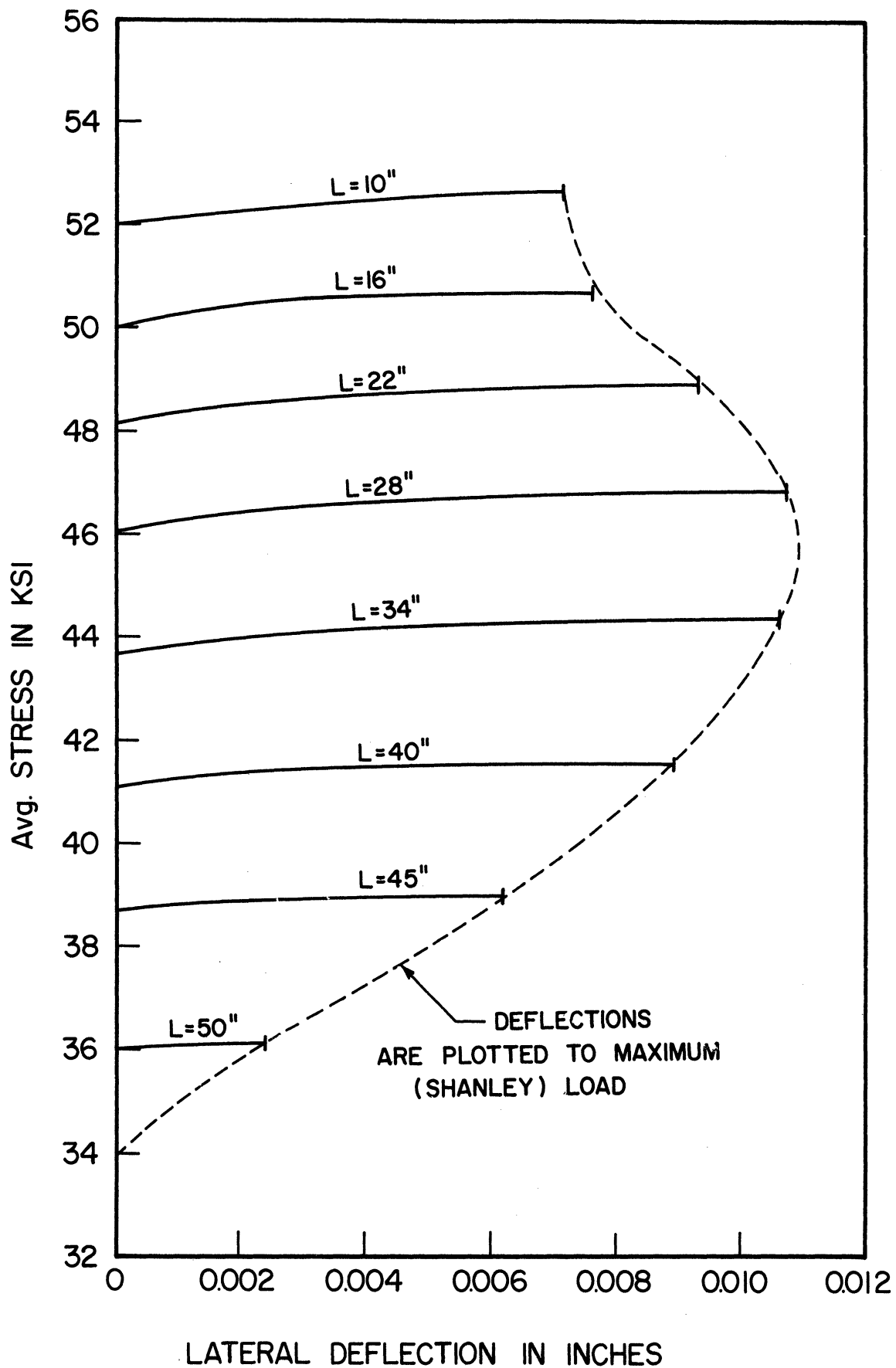


Figure 11. Lateral Deflection vs. Axial Load for Various Length Struts.

buckling will occur, and increases to a maximum in the intermediate column range.

For a particular length $L = 30$ inches, simulated tests were made in which the strut was held straight above the tangent modulus to various stress levels and then permitted to start bending. The suggestion for this type of test goes back to vonKármán's discussion of the second Shanley paper⁽¹⁾ in which, referring to the tangent modulus and reduced modulus loads, vonKármán stated

"...One can construct sequences of equilibrium positions starting from any load between the two limiting values corresponding to the tangent modulus and the reduced moduli. The inclination of the equilibrium lines representing the load as a function of the deflection is steepest for the line starting from the lower limiting load and becomes zero for the line starting from the upper limiting load (i.e. the reduced modulus load). Equilibrium lines have an envelope that starts from the lower limiting load and--at least as long as the stress strain curve can be considered straight and the deflection small--approaches asymptotically the load computed with the reduced modulus."

The foregoing comment accurately describes the initial portion of the load deflection curves shown in Figure 12. However,

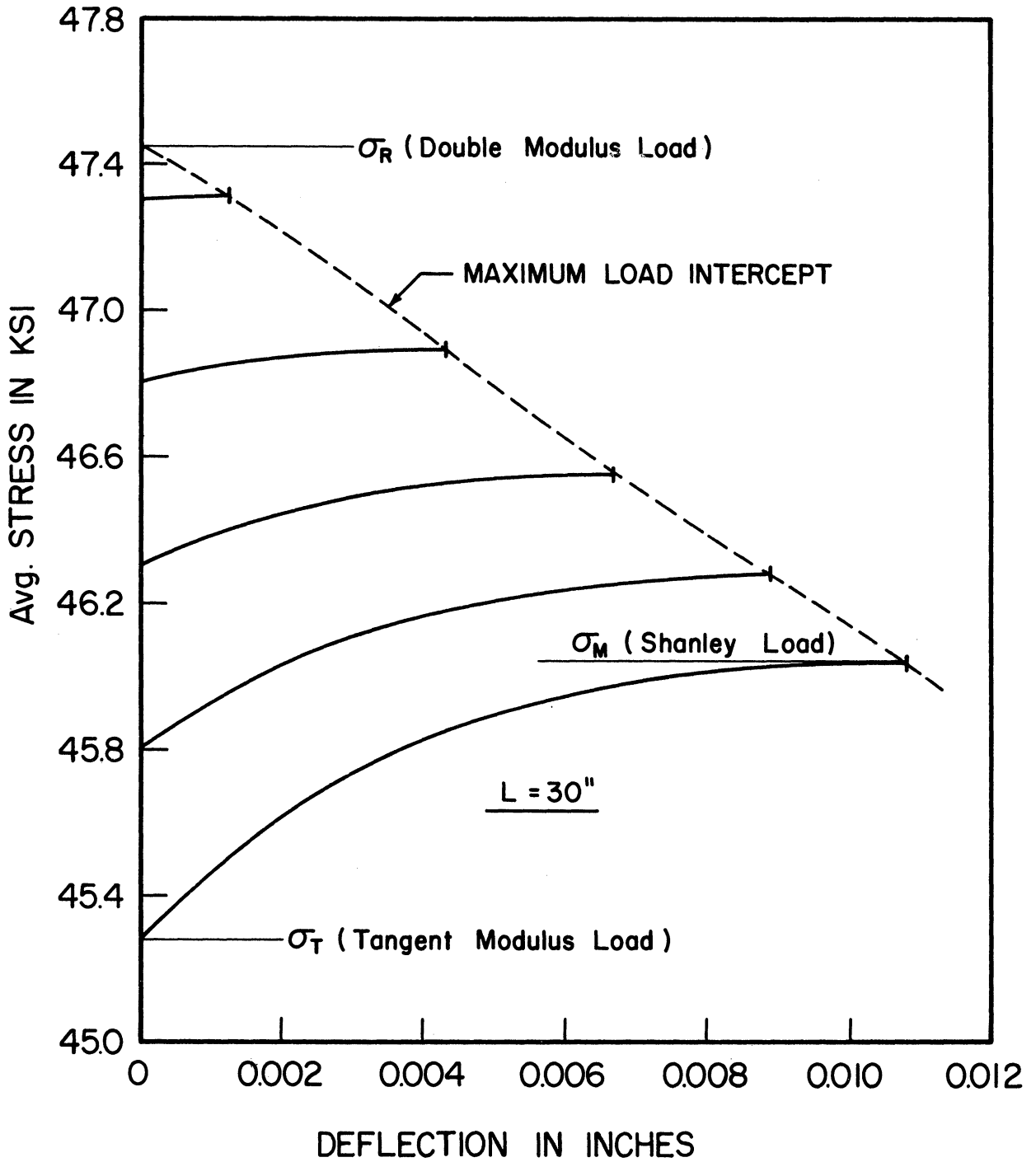


Figure 12. Lateral Deflection vs. Axial Load With Strut Held Straight to Various Stresses Above Tangent Modulus Load.

for the typical stress-strain curve used in this study, it is obvious that the comments regarding the asymptotic approach to the reduced modulus load have no real practical significance even though they are technically correct for that special case where the stress-strain curve would be straight above the tangent modulus load. If it were straight, of course, the reduced modulus load in the present case would be much greater than as calculated, as shown, at approximately 47.4 ksi, at which load the tangent modulus that determines the reduced modulus has substantially decreased from the tangent modulus at the tangent modulus load of about 45.3 ksi.

To demonstrate the different load-deflection behavior that results when the stress-strain curve remains straight above the tangent modulus ($E_t = \text{const.}$) load, Figure 13 should be compared with Figure 12.

In Figure 13 the curve of Figure 12 that determines the Shanley load (bending initiated at σ_t) is redrawn to a new scale. The pseudo σ_R based on E_t at the tangent modulus load is indicated and is seen to be greatly in error and much too large. Although not shown herein, this error progressively increases as the strut is made shorter. The great difference between behavior assuming constant E_t and predicted actual behavior leading to the Shanley load is graphically demonstrated. Whereas, with constant E_t , the lateral deflection and corresponding column load would both theoretically increase as much as the geometric limitations permit, the actual load differs but little from the tangent modulus load and the Shanley load is reached at extremely small lateral deflection.

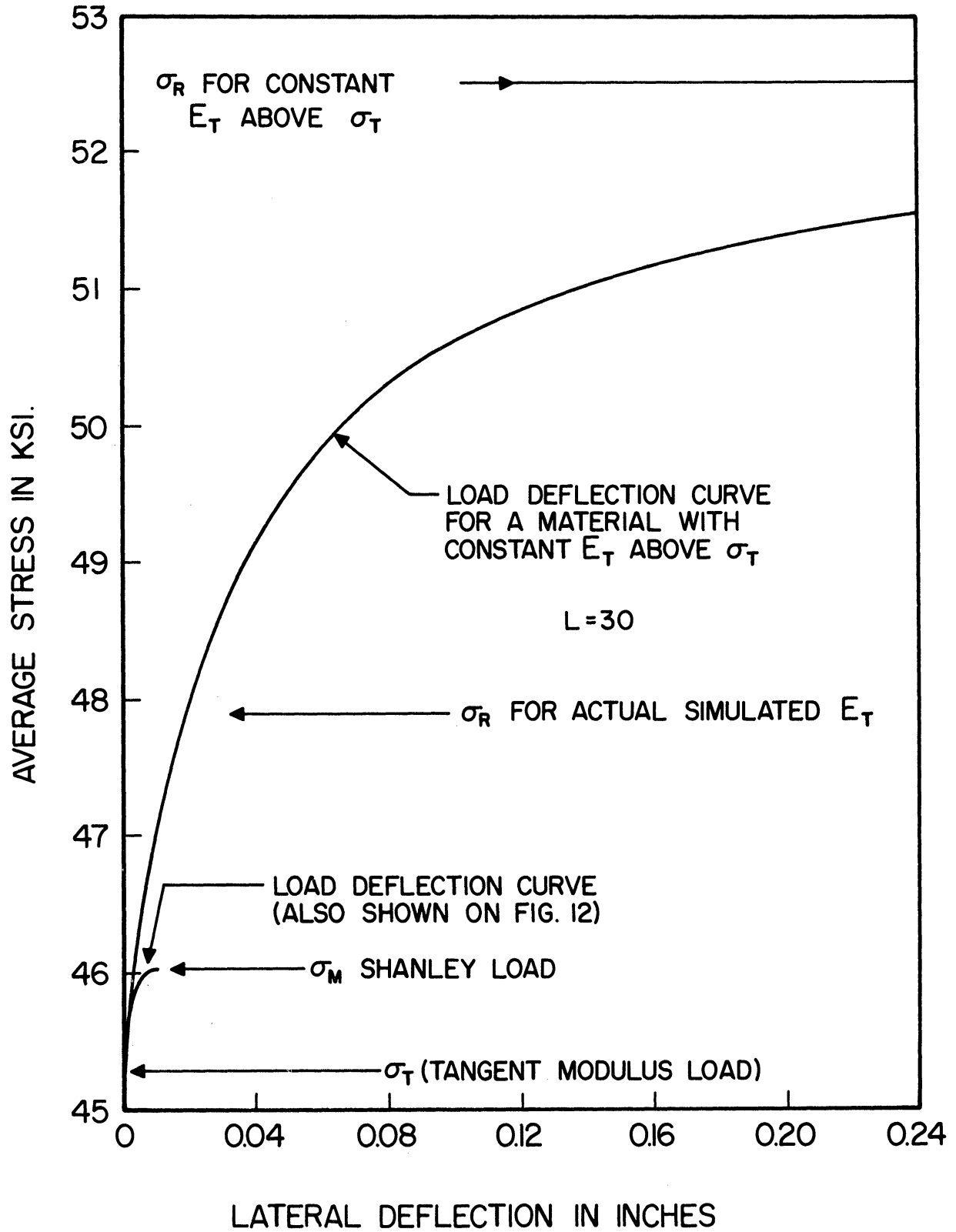


Figure 13. Lateral Deflection vs. Axial Load for Assumption of Constant E_T Above σ_T .

3.3 Column Strength Curve

Figure 14 shows the curve of strut length versus average stress (or load) at the various critical loads for the buckling model. These include the reduced modulus load, the maximum or Shanley load, and the tangent modulus load. Also, for comparative purposes, the reduced modulus load and tangent modulus load are given for a one inch by one inch column of constant section. The curves tend to join, as they should, at small lengths. Although the maximum or Shanley load is closer to the tangent modulus load than the reduced modulus load, no particular conclusion can be drawn from this relation since these simulated tests pertain to one particular material. The effort has not been so much to draw general conclusions, but rather, by a very close look at buckling behavior, lead to an improved understanding of what actually goes on between these various loads.

4. Summary

Although the simulated tests described herein have pertained to an inelastic buckling model with rigid bars adjacent to the center bending portion, it would be possible with minor changes in the computer program to simulate somewhat more nearly actual column behavior by some arbitrary assumption as to the distribution of M/EI along the column. This was not done because it was considered better to present a closely approximate solution of the model discussed herein rather than an incorrect solution of a more realistic representation of a column. The present work is simply one step along the way toward the

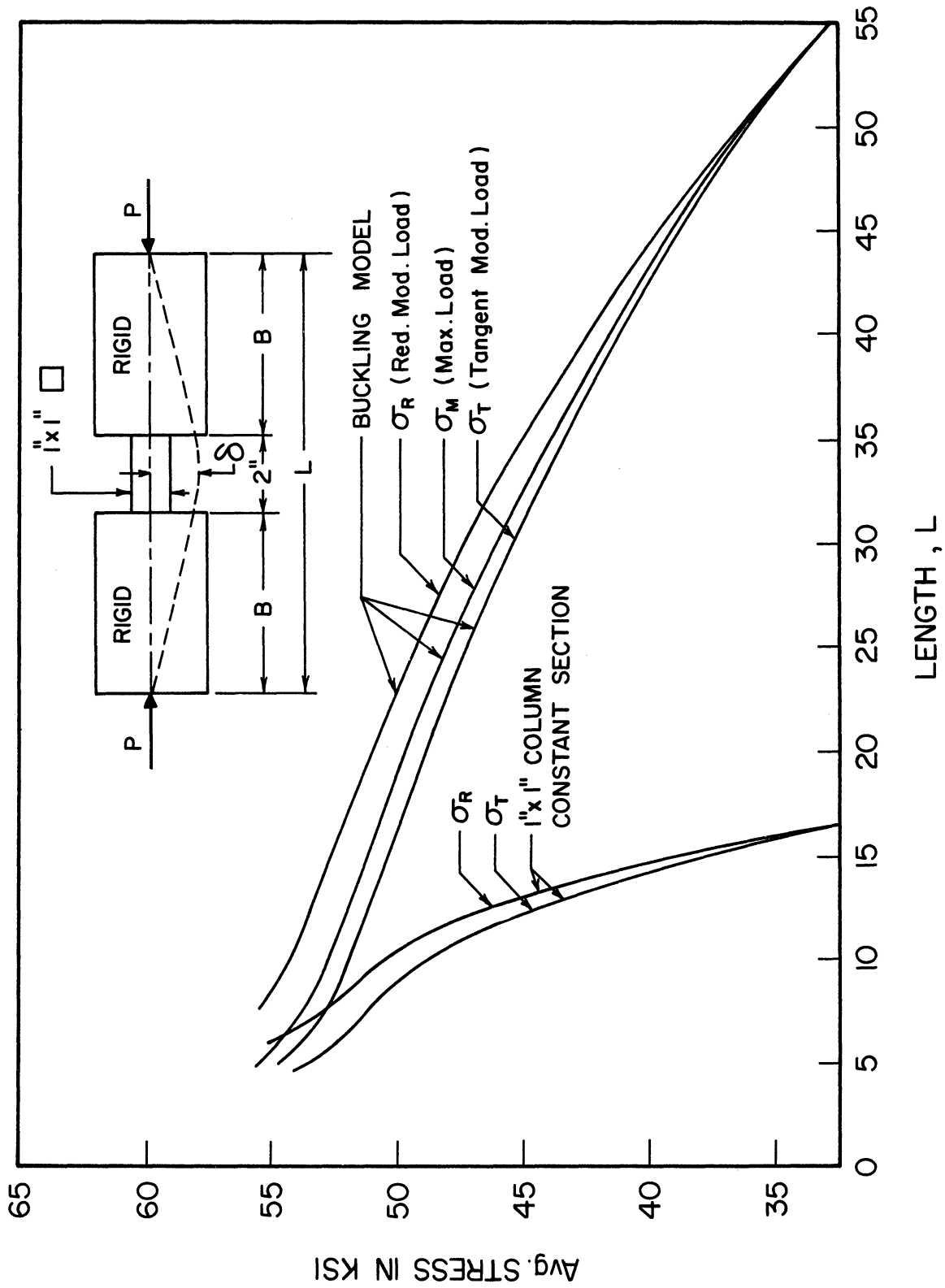


Figure 14. "Column" - Strength Curves.

projected solution of columns with variable cross section in the inelastic range with correct evaluation of the buckled shape at the various load levels above the tangent modulus load. In such a study errors in any assumed deflection configuration would be reduced by an iterative procedure making use of Newmark's⁽⁸⁾ numerical method as adapted to inelastic buckling.

It has been the aim of the present paper simply to improve understanding of buckling behavior in the inelastic range and to clarify some concepts that relate to Shanley's important contributions. On the basis of the simulated tests carried out in this study and described herein the following statements may be made. These statements are restricted to a material for which $\frac{d^2\sigma}{d\epsilon^2}$ is continuous and negative above the proportional limit.

1. The inward movement of the termination point of strain regression from the convex side of the column, immediately above the tangent modulus load, as predicted by Shanley in Figure 7 of Reference 1, has been reproduced quantitatively for a specific aluminum alloy within a localized rectangular cross sectional constriction in an otherwise rigid strut.
2. The procedure is simple in concept and the computer program can be adapted with minor alterations to any other stress-strain diagram or diagrams for which suitable mathematical expressions may be written.
3. The procedure presented herein is projected as the initial step toward the accurate evaluation of maximum inelastic

buckling loads for columns of variable cross section and arbitrary stress-strain properties.

4. In determining inelastic buckling equilibrium configurations and maximum loads above the tangent modulus load in members made of aluminum alloy it is essential to consider the continuing decrease of tangent modulus in the region of increasing compressive stress.
5. The assumption of bilinear elasticity as an approximation of inelastic stress-strain properties may in some instances lead to grossly erroneous results if inelastic stability is involved in the case of a material such as structural aluminum alloy.
6. If a column is constrained to remain straight in the inelastic range, above the tangent modulus load, it will reach a maximum load that is greater than the Shanley load and less than the reduced modulus load. The deflection at the maximum load will be progressively less as the reduced modulus load is approached.
7. The maximum or Shanley load for an ideal column of a typical structural aluminum alloy in the inelastic range is reached at relatively small deflections relative to the column breadth.
8. Further validation is given to the significance of the tangent modulus load as a proper basis for the evaluation of column design formulas and the double or reduced modulus

load is seen to be of no practical significance for materials typified by the stress-strain curve for structural aluminum alloy used herein.

5. References

1. Shanley, F. R., "Inelastic Column Theory," J. Aero Sci., Vol. 14, No. 5, May 1947, pp. 261-268, including discussion by T. vonKármán.
2. Hoff, N. J., "Buckling and Stability," J. Royal Aero. Soc., Vol. 58, Aero Reprint No. 123, Jan., 1954.
3. Column Research Council, "Guide to Design Criteria for Metal Compression Members," 1960, published by Column Research Council at the University of Michigan, Ann Arbor, Michigan.
4. Templin, R. L., Strum, R. G., Hartmann, E. C., and Holt, M., "Column Strength of Various Aluminum Alloys," Aluminum Research Laboratories, Technical Paper No. 1.
5. Shanley, F. R., "The Column Paradox," J. Aero Sci., Vol. 13, No. 5, Dec., 1946, p. 678.
6. Duberg, J. E. and Wilder, T. W., III, "Column Behavior in the Plastic Stress Range," J. Aero Sci., Vol. 17, No. 6, June 1950, pp. 323, see also NACA T.N. 2267, Jan., 1951.
7. Lin, Tung-Hua, "Inelastic Column Buckling," J. Aero Sci., Vol. 17, No. 3, March 1950, pp. 159-172.
8. Newmark, N. M., "Numerical Procedure for Computing Deflections, Moments, and Buckling Loads," Trans. ASCE, Vol. 108 (1943), pp. 1161 to 1234.
9. Ramberg, W. and Osgood, W. R., "Description of Stress-Strain Curves by Three Parameters," NACA T.N. No. 902, July 1943.